Raman studies in nanocrystalline lead (II) fluoride

2005 J. Phys.: Condens. Matter 17 863

(http://iopscience.iop.org/0953-8984/17/6/007)

INSTITUTE OF PHYSICS PUBLISHING JOURNAL OF PHYSICS: CONDENSED MATTER

J. Phys.: Condens. Matter **17** (2005) 863–874 doi:10.1088/0953-8984/17/6/007

Raman studies in nanocrystalline lead (II) fluoride

P Thangadurai[1], S Ramasamy[1,3] and R Kesavamoorthy[2]

[1] Department of Nuclear Physics, University of Madras, Guindy Campus, Chennai 600025, India
[2] Materials Science Division, Indira Gandhi Centre for Atomic Research, Kalpakkam 603102, India

E-mail: sinna_ramasamy@yahoo.com

Received 10 December 2004, in final form 11 January 2005
Published 28 January 2005
Online at stacks.iop.org/JPhysCM/17/863

Abstract

Nanocrystalline lead fluoride was prepared by an inert gas condensation technique under ultra-high vacuum conditions. Structural studies were carried out with x-ray diffraction analysis. As-prepared and vacuum annealed samples were found to contain both orthorhombic (α) and cubic (β) phases of PbF_2. The annealed samples contain dominantly the cubic phase. Grain sizes were found to be in the range from 21 to 43 nm. Raman scattering measurements have been performed on these samples in different frequency regions. Characteristic phonon vibrational modes such as T_{2g} for β-PbF_2 have been observed in addition to some modes corresponding to α-PbF_2. The Raman lines were assigned to β and α-PbF_2 on comparison with the already reported, both calculated and experimental, values. Some new modes have also been observed at the higher frequency region. The modes at higher frequencies were correlated to vibrations of electronic centres whose density varied with annealing temperature. The presence of electronic centres was investigated by photoluminescence studies. The widths of the Raman spectral lines were found to decrease with the increase in grain size. Low-frequency Raman studies revealed the presence of structural defect clusters. The defect cluster size was found to increase with annealing temperature.

1. Introduction

Lead fluoride is an optically transparent insulator crystallizing in the fluorite structure which consists of three interpenetrating face centred cubic lattices displaced along the body diagonal. Lead (II) fluoride exists in two structural phases. One is the orthorhombic α-PbF_2 and the other is the cubic fluorite structured β-PbF_2. These phases are very susceptible to high pressure and temperature. α-PbF_2 can be converted into β-PbF_2 by heating the former at 700 K for 1 h [1, 2], and the reverse can be achieved by applying high pressure of the order of

[3] Author to whom any correspondence should be addressed.

0.4 GPa [2]. Even though these two phases are fluorine ion conductors at room temperature, comparatively β-PbF_2 is a superionic conducting phase [3]. Also, the β-PbF_2 phase shows an interesting phenomenon called 'sublattice melting' at ~700 K. At this temperature, the fluorine ion sublattice melts and creates a large number of defects by leaving its site, and the compound displays enormous conductivity [4]. This is called the superionic conducting state [4]. Due to this phenomenon there is an anomaly in the specific heat [5] and dielectric constant [6] of this material near this temperature. Because of its high ionic conductivity, β-PbF_2 is used as a solid electrolyte in solid-state batteries.

Raman spectroscopy is a non-destructive and sensitive tool for determining the local atomic arrangements and vibrations, and it has been used to characterize nanocrystalline materials [7]. Also, this technique has been used to identify oxygen vacancies in solid solutions with the fluorite lattice [8]. The frequency of Raman lines depends upon the lattice parameters and thus is a function of temperature and pressure. The linewidth provides information not only about the phonon decay but also about the lattice distortion, a possible distribution of force constant. It is also a powerful tool for analysing the crystallographic size effects in dielectrics [9]. Fluorite structure based compounds have been studied using Raman spectroscopy by many researchers. Kolesik *et al* [10] have studied low-frequency vibrational modes in fluorite based superionic conductors. Disorder in the anion sublattice is an important phenomenon in fluorite structured PbF_2 and has been studied by Raman scattering by Hayes *et al* [11]. In general, PbF_2 crystallizes in the fluorite structure with O_h^5 symmetry. It has a Raman active mode with $k = 0$ referred to as T_{2g}, a triply degenerate mode. In this T_{2g} mode, the cation lattice is stationary, whereas the anions undergo displacement against each other and against the cation lattice [12]. Krishnamurthy and Soots [13] have studied the first-order Raman scattering in PbF_2 single crystals at different temperatures. Also, a good description was given for the Raman spectra of α-PbF_2 by calculating the interatomic potential parameters based on the shell model by Sahni and Jacobs [14].

Even though much work has been done on single crystals of PbF_2, nanocrystalline PbF_2 has not been studied thoroughly yet to the best of our knowledge. Nowadays the field of nanoscience and nanotechnology has been at the cutting edge of research because of the novel properties of nanomaterials [15]. In this work, we report Raman spectroscopy results on nanocrystalline PbF_2. The observed Raman modes are compared with the experimentally observed values as well as the calculated values in the literature. In addition, some extra vibrational modes have also been observed and they are correlated to the existence of electronic centres in the samples.

2. Experimental procedure

Nanocrystalline PbF_2 was prepared by an inert gas condensation technique using an ultra-high vacuum chamber, which was designed and fabricated indigenously. High-purity (99.99%) PbF_2 (Sigma Chemicals Company, Inc., USA) was loaded in a molybdenum (Mo) boat inside the chamber, which was evacuated down to a pressure of 5.7×10^{-8} mbar. With a high-purity helium (He) environment acting as a carrier gas, the precursor was evaporated by joule heating and the nucleated nanoclusters were deposited on a cold finger kept at 77 K. Details of the method of preparation have been discussed elsewhere [16]. The as-prepared sample was annealed, under a vacuum of 2×10^{-6} mbar, at different temperatures (423, 473, 573, 623 and 673 K) to get different grain sizes. Structural studies of these PbF_2 samples were performed using x-ray diffraction (XRD). The XRD patterns were recorded using a Seifert powder x-ray diffractometer with Cu $K\alpha_1$ radiation. The grain sizes of all these samples were estimated from the full width at half maximum (FWHM) of the XRD peak using the Scherrer formula.

Pellet samples were used for Raman measurements. The Raman spectra were recorded at room temperature in the backscattering geometry. The vertically polarized 488 nm line of an argon ion laser with 200 mW power was used as an exciting source. The back-scattered light from the sample was dispersed using a double monochromator SPEX, model 14018, and detected using a thermoelectrically cooled photomultiplier tube (FW ITT 130) operated in the photon counting mode. Scanning of the spectra and data acquisition were carried out using a microprocessor-based data acquisition cum control system. Raman spectra were recorded in two regions: one from 50 to 350 cm^{-1} and the other from 700 to 1100 cm^{-1} at 1 cm^{-1} intervals with 10 s integration time and 4.2 cm^{-1} instrument resolution. Low-frequency Raman spectra were recorded with the same laser line of 100 mW power in the frequency range from 5 to 40 cm^{-1} at 10 s integration time in steps of 0.5 cm^{-1} with 1 cm^{-1} instrument resolution. The photoluminescence spectra were recorded with the same laser beam in steps of 20 cm^{-1} with 2 s integration time and 4.2 cm^{-1} instrument resolution.

An x-ray photoelectron spectroscopy (XPS) study was performed to verify the presence of lead clusters in these samples. The XPS system used for this study was a VG ESCALAB MK200X system, with 150 mm hemispherical analyser. The spectra were collected using an Al Kα x-ray source and with 20 eV pass energy of the analyser. The data acquisition and processing were carried out using Eclipse software. The instrument was calibrated with the Au $4f_{7/2}$ line at 84.0 eV with 1.6 eV FWHM. The 1s peak of carbon was taken at 285.0 eV for the charging correction.

3. Results and discussion

Figure 1 gives the x-ray diffraction patterns for nanocrystalline PbF_2 annealed at different temperatures. The grain sizes are found to be in the range from 21 to 43 nm. As-prepared and annealed PbF_2 contain both α- and β-phases of PbF_2. But the samples annealed at or above 473 K contain β-phase as the dominant phase with a very small quantity of α-phase.

All fluorite structured materials (like CaF_2) belong to the O_h^5 space group. The symmetries of the normal modes of the vibrations of the three atoms in the unit cell are given by the various irreducible representations of the O_h point group: $2F_{1u} + T_{2g}$. The zone-centre fundamental modes of this structure can be classified as a triply degenerate acoustic mode (F_{1u}), a triply degenerate IR active optical mode (F_{1u}), and a triply degenerate Raman active mode (T_{2g}). Raman scattering in divalent fluorides has been rigorously studied by Kessler *et al* [17] under different pressures and at different temperatures. They have observed Raman vibrational modes experimentally for BaF_2 and α-PbF_2. They have assigned those modes by comparing them with the available literature and with the predictions derived from some simple models of the lattice dynamics of ionic materials.

Figure 2 shows typical Raman spectra for as-prepared and 623 K annealed nanocrystalline PbF_2 and its inset is the low-frequency Raman spectrum for the former. The Rayleigh tail background in our samples is very high, as shown in figure 2, since our nanograin samples made into pellets have a large number of grain boundaries which Rayleigh-scatter the incident light. However, the Raman peaks riding in this background are very clear and were analysed with the PEAKFIT subroutine. As these samples contain both the phases, we will discuss the results in the order of β- and then α-phase. A mode is observed at 256 cm^{-1} which can be assigned to the Raman active T_{2g} symmetry mode by comparing with the earlier reported value of 258 cm^{-1} in β-PbF_2 [17, 18]. Because of its weak intensity, it has been plotted separately in figure 3. This peak actually arises from the triply degenerate T_{2g} lattice mode and this is a characteristic peak for β-PbF_2. Because of the vibration of fluorine ions in this mode, this was used to study the fluorine sublattice melting in PbF_2 by Valakh *et al* [18]. During sublattice

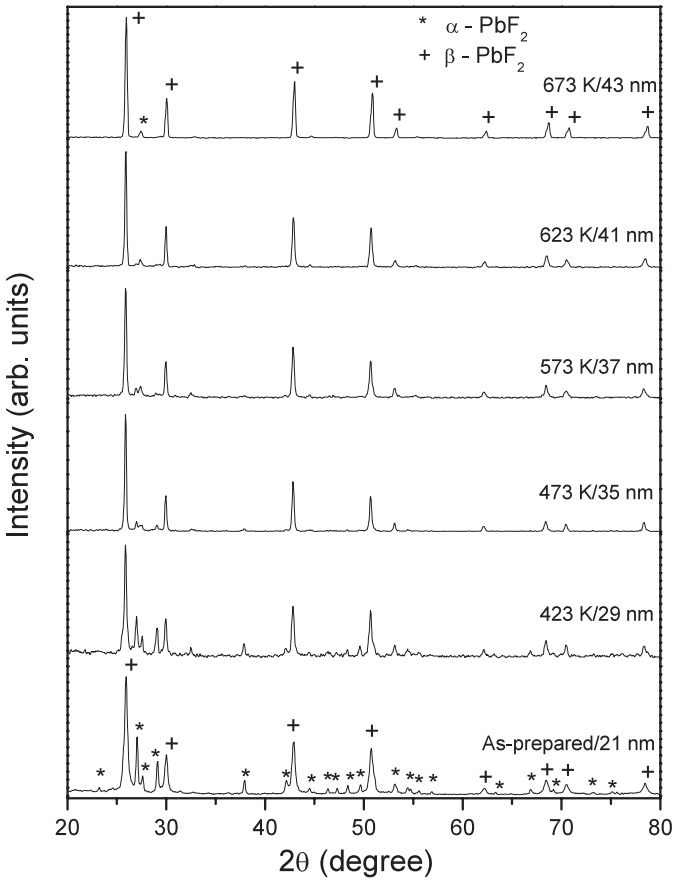

Figure 1. XRD patterns for nanostructured PbF_2 with different annealing temperatures and grain sizes. The annealing temperature and grain size are given against the corresponding pattern (+ refers to β-PbF_2; $*$ refers to α-PbF_2). Isochronal annealing was done under vacuum for 1 h.

melting near 700 K, the anions (fluorine ions) will leave their site to wander in the cation lattice. Therefore, this change in position of anions will influence the T_{2g} Raman mode. Valakh *et al* [18] have observed that the width of the T_{2g} mode increased considerably on increasing the temperature due to sublattice melting, and the frequency of vibration at 540 K decreased to 247 from 258 cm^{-1} at 100 K. In the present case, the Raman frequency of the T_{2g} mode increases marginally from 250 cm^{-1} for 21 nm grain size to 256 cm^{-1} for 41 nm grain size, as shown in figure 3. However, this frequency decreases drastically to 240 cm^{-1} after annealing at 673 K (43 nm grain size). In order to verify whether this blueshift in Raman frequency from 250 to 256 cm^{-1} is due to lattice expansion, the lattice parameters have been obtained from the XRD data (figure 1) and the change in unit cell volume with grain size is given in figure 4 for the α- and β-phases. It is observed that the unit cell volume decreases with the increase in grain size. Similar observations have been reported in the literature for nanocrystalline materials, and the increase in lattice parameter can be explained by increased concentrations of defects with decreasing grain size [19]. The decrease in unit cell volume of the β-phase (figure 4) will result in the blueshift of Raman frequency which is in agreement with our observation for 21–41 nm grain sized samples (figure 3). However, the unit cell volume decreases drastically

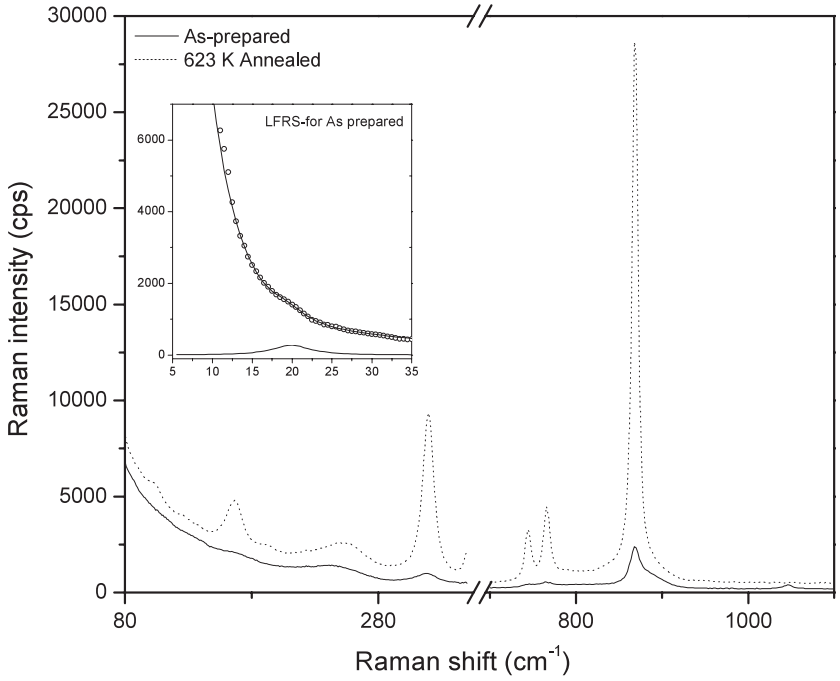

Figure 2. Raman spectra of as-prepared and 623 K annealed nanocrystalline PbF_2. The inset figure gives the low-frequency Raman (LFR) spectrum for as-prepared PbF_2; dots are the experimental data, and the continuous curve is the fit to a Lorentzian (given separately in the inset) and an exponential background.

(figure 4) after annealing at 673 K. The reason for the drastic redshift of T_{2g} frequency for the 673 K annealed sample is not clear, at present.

In figure 2, two more Raman modes are observed at 104 and 167 cm^{-1}. Assigning these modes should be done carefully in this case, because both the phases co-exist. The mode at 104 cm^{-1} has not appeared in as-prepared, 423 and 473 K annealed PbF_2. There is a possibility that this mode could have been originated from the disorder in the fluorite lattice [10]. But, in nanocrystalline PbF_2 annealed at higher temperatures, the intensity of this mode rises. Usually, the amount of disorder in a material decreases with high-temperature heat-treatment and hence the intensity should decrease and not increase as in this case. Therefore we cannot assign this mode to any disorder-type modes. Apart from the T_{2g} mode, there are no more Raman active modes in β-PbF_2. Hence, we have to consider the α-phase and its Raman active modes at this moment. Actually, Kessler *et al* [17] have predicted Raman vibrational modes for α-PbF_2 using rigid-ion calculations and compared their experimentally observed modes with the calculated values. With 12 atoms in the primitive cell, 36 normal modes are expected at the Γ point of the Brillouin zone. Among these $6A_g$, $6B_{1g}$, $3B_{2g}$ and $3B_{3g}$ are expected to be Raman active. No experimental vibrational spectra for orthorhombic lead fluoride were found in the literature before the report of Kessler *et al* [17]. We have taken the calculated values for α-PbF_2 from Kessler's work and compared the observed Raman modes. The possibility for the 104 cm^{-1} mode is the calculated B_{1g} mode of α-PbF_2 reported at 108 cm^{-1} [17]. Maybe this mode appears only for the samples annealed at 573, 623 and 673 K due to increased crystallinity.

Similarly the other mode observed at 167 cm^{-1} can be assigned to the A_g symmetry mode of α-PbF_2. Its equivalent calculated and observed modes are at 151 and 172 cm^{-1}

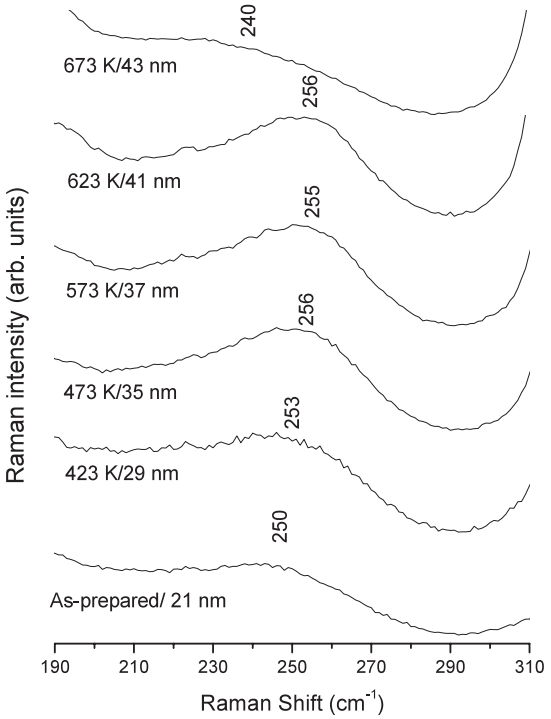

Figure 3. The Raman line at 256 cm^{-1} corresponds to the T_{2g} vibration mode of nanocrystalline β-PbF_2. The annealing temperature and the grain size are given against each pattern.

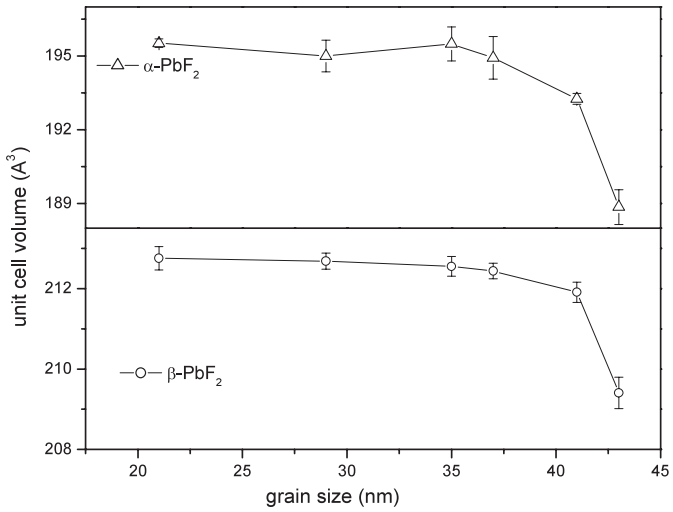

Figure 4. Variation of unit cell volume with grain size in nanocrystalline PbF_2. The curve is a guide to the eye.

respectively [17]. Another Raman mode observed at 318 cm^{-1} can be assigned to the B_{1g} mode of α-PbF_2, for which the calculated value by Kessler is 316 cm^{-1}. This mode shows very good agreement with the reported value. The variation of the full width at half maximum

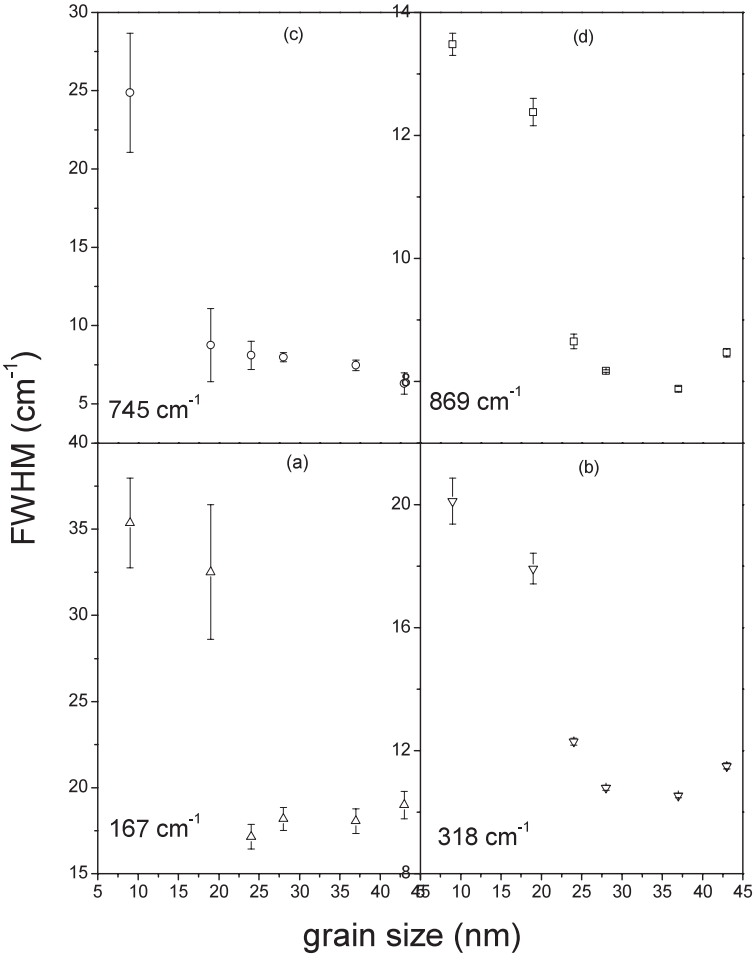

Figure 5. Variation of full width at half maximum of typical Raman peaks with grain size for nanocrystalline PbF_2. The peak frequencies are (a) 167, (b) 318, (c) 745 and (d) 869 cm^{-1}, given against each plot.

(FWHM) of the 167 and 318 cm^{-1} Raman modes is given in figures 5(a) and (b). The width decreases with the increase in grain size in both cases, and this may be due to higher grain size resulting in good crystallinity [20].

In addition to the regular Raman modes discussed above, four new modes are observed at 745, 766, 869 and 1045 cm^{-1} in the frequency region between 700 and 1100 cm^{-1}, and they have not been reported in the literature so far. These spectra are given in figure 6. These modes are interpreted in the following way. The possible calculated Raman modes in both phases of PbF_2 have been reported below 316 cm^{-1} (the observed values are below 292 cm^{-1}) [17]. But the newly observed Raman frequencies are above 700 cm^{-1}. Therefore these modes are not regular lattice modes of PbF_2. The inset of figure 6 shows the Raman peak observed at 1045 cm^{-1}. It is interesting to note that this peak is well pronounced only in as-prepared and 423 K annealed samples, and it does not appear in the other high-temperature annealed samples. In contrast, the other three modes have become intensified with annealing temperature in all the samples. One may suspect the presence of some other impurity phase,

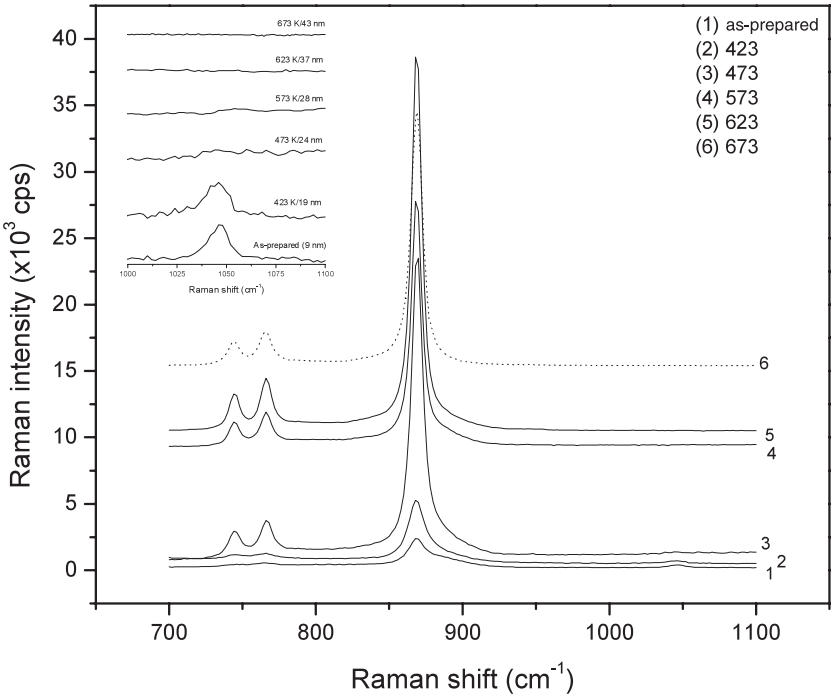

Figure 6. Raman spectra for nanocrystalline PbF_2 measured in the range 700–1100 cm^{-1}. The vertical scale was shifted in order to avoid overlapping of peaks. The inset figure shows the Raman peak at 1045 cm^{-1} observed only in the smaller grain sized samples.

such as lead oxide, producing these modes. But no signature of oxides of lead is found in the XRD and XPS. (It should be noted that the annealing was done under a vacuum of the order of 10^{-6} Torr.) So, there may be a correlation between the intrinsic properties and the annealing temperature. A photoluminescence (PL) study has been carried out for all the samples. The PL spectra for nanocrystalline PbF_2 with different annealing temperatures are given in figure 7. It can be observed from figure 7 that the intensity of the PL spectra increases up to 473 K annealed samples and then decreases. This PL might be due to electronic centres. The number density of the electronic centres increases up to 473 K and then decreases at higher annealing temperatures. We propose that the formation of electronic centres in the samples may give rise to these Raman modes at high frequencies. The fluorine ion might have left its site leaving one electron to its site and become neutral in the interstitials. Thus it forms electronic centres in nanocrystalline PbF_2. The vibrations of the bonded electronic centres with Pb^{2+} ion might give rise to the high-frequency Raman modes. Raman scattering by electronic centres (F centres) has been theoretically studied by Benedek and Nardelli [21] in ionic crystals such as NaCl and KCl. They have found that the calculated Raman shifts of electronic centres lie around 1000 cm^{-1}, and the theory agrees very well with the experimentally observed Raman shift. Recently Spanier *et al* [22] have studied the grain size dependence of Raman scattering in CeO_{2-y}. The system will contain large amount of vacancies. In order to explain the observed peak shifts, they have used different available models and found satisfactory agreement with the observed data. However, they have also found a new Raman shift at 830 cm^{-1}, which they have concluded as being due to either a second-order phonon, a local mode centred at vacancies, or the presence of another elemental species. These studies support the argument

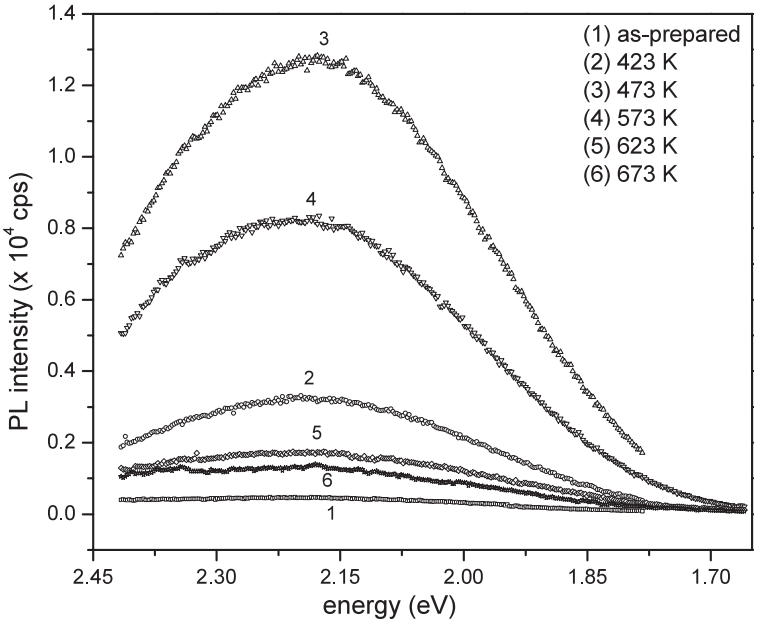

Figure 7. Photoluminescence spectra of nanocrystalline PbF_2 annealed at different temperatures.

that these high-frequency Raman modes are due to electronic centres. Figures 5(c) and (d) show the variation of FWHM of the observed Raman modes centred at 745 and 869 cm^{-1}. The decrease in width with grain size is due to higher crystallinity.

Figures 8(a) and (b) show the typical LFR spectra for nanocrystalline PbF_2. All the LFR spectra were fitted with an exponential background and a Lorentzian line shape. In these figures, the solid curves are the fits. All the samples show only one low-frequency Raman peak. Usually, one can observe low-frequency peaks of Raman spectra in vitreous materials. Because of the cubic structure of fluorite based superionic conductors, these peaks are unexpected. However, it is known that these materials are highly disordered and their vibrational properties are similar to those of the amorphous solids [23]. Low-frequency Raman spectra of disordered and amorphous materials often contain a broad peak, usually called the boson peak, at around 30 cm^{-1} [24]. There are some reports stating that the spectral form of the boson peak is the same for various glasses independent of the chemical composition [10]. In particular, fluorite based superionic conductors show a low-frequency Raman peak with larger width [10] (approximately 20 cm^{-1}). The LFR spectra of PbF_2 show peaks at much lower frequencies (<20 nm^{-1}) with FWHM of almost 4–7 cm^{-1}. Mostly, low-frequency Raman modes have been used to identify the presence of metallic clusters such as Ag in the insulating matrix like ZrO_2 [25] and SiO_2 [26]. In these works [25, 26], the authors have calculated the metallic cluster size from the peak frequency of the LFR spectra. As far as metals or semiconductor nanoclusters are concerned, confined acoustic phonons on their surface give rise to low-frequency vibrational modes. The low-frequency Raman scattering from a nanocluster is due to an elastic vibration of the nanocrystal itself. These low-frequency modes may arise from the vibration of a spherical or ellipsoidal grain. In the present samples, one may expect the presence of Pb metallic nanoclusters in the PbF_2 matrix. The reason for this cluster existence may be unbridged cations. In order to verify whether the LFR spectrum peaks emerge from the Pb nanoclusters or not, x-ray photoelectron spectroscopic measurements have

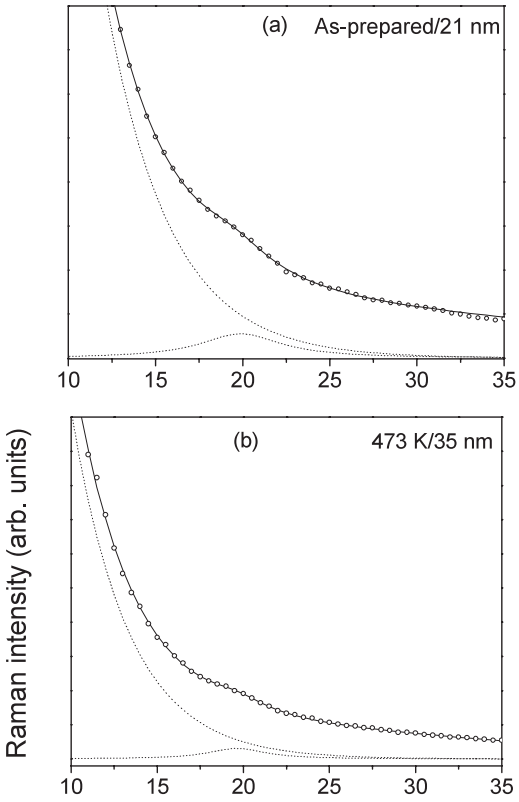

Figure 8. Typical low-frequency Raman spectra for nanocrystalline PbF_2 with different grain sizes. The annealing temperature and the grain size are given at the right corner of each figure. Solid curves are the fitted curves. The low-frequency Raman spectra are fitted with an exponential background and a Lorentzian line shape.

been carried out. Typical x-ray photoelectron spectra for the as-prepared and 473 K annealed PbF_2 are given in figure 9 for the Pb $4f_{7/2}$ state. The reference binding energy for Pb $4f_{7/2}$ is 138.8 eV. The observed binding energy for Pb $4f_{7/2}$ is 138.4 and 138.8 eV for as-prepared and 473 K annealed PbF_2 respectively. Also, from the full width at half maximum of the peaks, it can be observed that the compound contains only PbF_2 and there is no signature of the presence of Pb–Pb nanoclusters and oxides of Pb. Therefore, the possibility of the presence of Pb clusters and lead oxide(s) in these samples is ruled out.

Low-frequency vibrational modes in fluorite based doped superionic conductors have been studied by Kolesik *et al* [10]. They have interpreted the LFR spectra data in terms of the vibrational modes localized on structural defects. They have observed low-frequency modes at a peak frequency varying from 30 to 62 cm^{-1} due to dopant clusters or defect regions in these materials exhibiting quasi-localized low-frequency resonant modes. The short-range order in doped fluorites may be described by the formation of various clusters consisting of dopant ions, fluorine interstitials and vacancies. We do not have any dopants in our samples. But nanocrystalline PbF_2 may contain defects such as anion vacancies and fluorine interstitials. Hence there is a probability that these defects may form small clusters. The interstitial fluorine ion might have formed into clusters to give rise to low-frequency modes. The size of these defect clusters may vary from one sample to the other due to many parameters such as grain

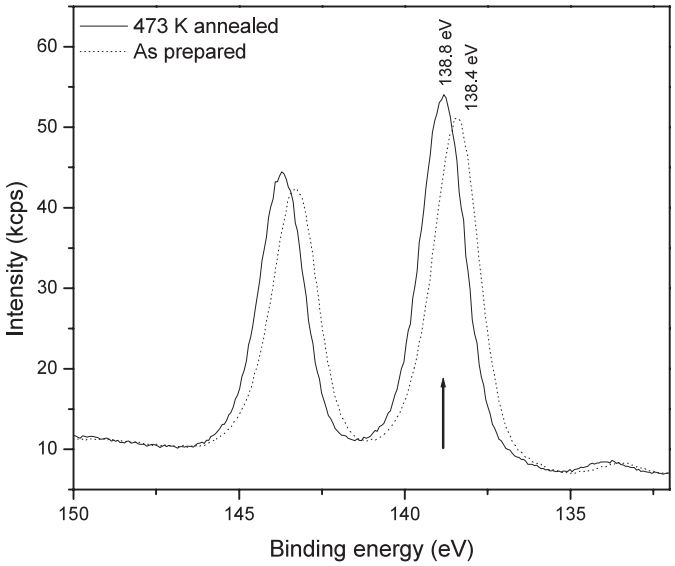

Figure 9. X-ray photoelectron spectra of the Pb $4f_{7/2}$ state (marked with the arrow) for the as-prepared and 473 K annealed nanocrystalline PbF_2.

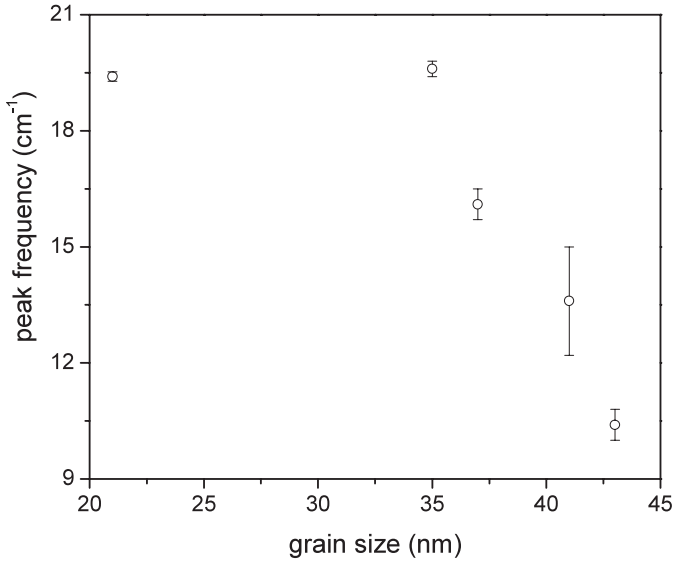

Figure 10. Variation of the peak maximum of the low-frequency Raman vibrational mode in nanocrystalline PbF_2 as a function of grain size.

size, annealing conditions, etc. It is known [10] that the size of a defect cluster is inversely proportional to the peak frequency. Figure 10 shows the variation of the peak frequency of the low-frequency Raman modes of nanocrystalline PbF_2 as a function of grain size. It is observed that the peak frequency of this mode decreases with the increase in grain size. Since the size of the defect cluster is inversely proportional to the peak frequency, it is observed that the defect cluster size increases with annealing temperature. This may by due to the thermally enhanced

diffusion of defects and that they have become clustered. The LFR spectrum peak width is a little high (∼4–7 cm^{-1}) indicating that there is a wide distribution of defect cluster size in the sample.

4. Conclusion

Nanocrystalline PbF_2 with different grain size has been studied by XRD, Raman spectroscopy and XPS. The characteristic mode of β-PbF_2, T_{2g}, and modes such as A_g and B_{1g} of α-PbF_2 have been observed. In addition to these, four new vibrational modes have been observed which are assigned to the vibrations of the electronic centres formed in these nanocrystalline samples. In order to establish the presence of electronic centres, a photoluminescence study has been done and reported. The Raman linewidth of the vibrational modes decreases with the increase in grain size due to the increase in crystallinity. Low-frequency Raman studies showed an increase in the defect cluster size with annealing temperature.

Acknowledgments

DST (Scheme No. SR/S5/NM-58/2002), UGC-COSIST and UGC-SAP, India are acknowledged. Dr B Purniah, Dr S V Narasimhan, Dr S Bera and Mr T Saravanan of IGCAR, Kalpakkam are gratefully acknowledged for the XPS measurements. One of the authors (PT) acknowledges the CSIR, India for the award of SRF (9/115(565)/2002-EMR-I).

References

[1] Schoonman J, Ebert L B, Hsieh C H and Huggins R A 1975 *J. Appl. Phys.* **6** 2873
[2] Samara G A 1979 *J. Phys. Chem. Solids* **40** 509
[3] Samara G A 1977 *Ferroelectrics* **17** 357
[4] Derrington C E and O'Keeffe M 1973 *Nat. Phys. Sci.* **246** 44
[5] Volodkovich L M, Petrov G S, Vecher R A and Vecher A A 1985 *Thermochim. Acta* **88** 497
[6] Palchoudhuri S and Bichile G K 1988 *Solid State Commun.* **67** 553
[7] Chen Z, Tan S, Zhang S, Wang J, Jin S, Zhang Y and Sekine H 2000 *Japan. J. Appl. Phys.* **39** 6293
[8] Lin X M, Li L P, Li G S and Su W H 2001 *Mater. Chem. Phys.* **69** 236
[9] Schrever D, Waschk V and Chatelain A 1981 *Surf. Sci.* **106** 336
[10] Kolesik M, Tunega D and Sobolev B P 1992 *Solid State Ion.* **58** 237
[11] Hayes W, Rushworth A J, Ryan J F, Elliot R J and Kleppmann W G 1977 *J. Phys. C: Solid State Phys.* **10** L111
[12] Srivastava R, Lauer H V Jr, Chase L L and Bron W E 1971 *Phys. Lett.* A **36** 333
[13] Krishnamurthy N and Soots V 1970 *Can. J. Phys.* **48** 1104
[14] Sahni V C and Jacobs P W M 1983 *J. Phys. C: Solid State Phys.* **16** L241
[15] Nazarov A A and Mulyukov R R 2003 *Handbook of Nanoscience, Engineering and Technology* ed W A Goddard, D W Brenner, S E Lyshevski and G J Iafrate (New York: CRC Press) pp 22-1–41
[16] Thangadurai P, Ramasamy S and Manoharan P T 2004 *Eur. Phys. J.* B **37** 425
[17] Kessler J R, Monberg E and Nicol M 1974 *J. Chem. Phys.* **60** 5057
[18] Valakh M Ya, Kosatskii K, Litvinchuk A P and Azhnyuk Yu N 1984 *Sov. Phys.—Solid State* **26** 1382
[19] Zhang F, Chan S W, Spanier J E, Apak E, Jin Q, Robinson R D and Herman I P 2002 *Appl. Phys. Lett.* **40** 127
[20] Iqbal Z and Veprek S 1982 *J. Phys. C: Solid State Phys.* **15** 377
[21] Benedek G and Nardelli G F 1967 *Phys. Rev.* **154** 872
[22] Spanier J E, Robinson R D, Zhang F, Chan S-W and Herman I P 2001 *Phys. Rev.* B **64** 245407
[23] Gahill D G and Pohl R O 1989 *Phys. Rev.* B **39** 10477
[24] Mamedov S, Kisliuk A and Quitmann D 1998 *J. Mater. Sci.* **33** 41
[25] Govindaraj R, Kesavamoorthy R, Mythili R and Viswanathan B 2001 *J. Appl. Phys.* **90** 958
[26] Gangopadhyay P, Kesavamoorthy R, Nair K G M and Dhandapani R 2000 *J. Appl. Phys.* **88** 4975